Ion-Dependent Dynamics of DNA Ejections for Bacteriophage λ

David Wu,[†△] David Van Valen,[†△] Qicong Hu,[‡] and Rob Phillips[†*]
[†]Division of Engineering and Applied Sciences, California Institute of Technology, Pasadena, California; and [‡]Department of Biology, Stanford University, Stanford, California

ABSTRACT We studied the control parameters that govern the dynamics of in vitro DNA ejection in bacteriophage λ. Previous work demonstrated that bacteriophage DNA is highly pressurized, and this pressure has been hypothesized to help drive DNA ejection. Ions influence this process by screening charges on DNA; however, a systematic variation of salt concentrations to explore these effects has not been undertaken. To study the nature of the forces driving DNA ejection, we performed in vitro measurements of DNA ejection in bulk and at the single-phage level. We present measurements on the dynamics of ejection and on the self-repulsion force driving ejection. We examine the role of ion concentration and identity in both measurements, and show that the charge of counterions is an important control parameter. These measurements show that the mobility of ejecting DNA is independent of ionic concentrations for a given amount of DNA in the capsid. We also present evidence that phage DNA forms loops during ejection, and confirm that this effect occurs using optical tweezers.

INTRODUCTION

Bacteriophages have played a key role in the emergence of both molecular and physical biology. They were an essential component of the Hershey-Chase experiment (1), which established that DNA is the molecule of inheritance, and have since provided an important technology for cloning and protein expression (2). Phages have also been shown to be important model organisms for studies of macromolecular self-assembly, and the assembly of viruses from their constituent components in vitro was recently demonstrated (3). Bacteriophages have also been instrumental in the field of systems biology, as evidenced by the dissection of the transcriptional program responsible for the lysis-lysogeny decision (5–9). Finally, bacteriophages have played an important role in the field of single-molecule biophysics, as evidenced by single-phage packaging experiments that revealed the large (many pico-Newton) forces generated by motors that package phage DNA into protein capsids (4). Studies of the bacteriophage life cycle have yielded much insight in the physical biology setting, and we anticipate that it will continue to serve as a useful model system.

Here, we highlight four recently developed experimental techniques that can be used to examine how phage DNA is packaged into and released from protein capsids. These four techniques include single-molecule packaging of DNA, single phage ejection measurements, osmotic suppression of DNA ejection, and cryoelectron tomography of partially packed phages. In previous studies, single-molecule DNA packaging experiments were used to elucidate the mechanics of how DNA gets packaged into the capsid, and optical tweezers were used to make systematic measurements of the packaging force for phage λ and ϕ29 in a variety of different salt conditions (10). These experiments demonstrated that when the charge of the salts is increased, the genome is packaged at a higher velocity, and the internal force of the capsid DNA that resists packaging increases monotonically with a reduction in the charge of the salts.

These packaging experiments were complemented by single-phage ejection experiments in which phages were coerced into ejecting their DNA by the addition of a trigger protein and then observed under a microscope with the aid of flow and DNA staining dyes (11,12). These experiments illustrated the dynamics of the ejection process and provided some insight into the frictional forces experienced by the DNA as it exits the capsid (12–14). The principal quantity measured in these experiments is the velocity of ejection as a function of the quantity of DNA inside the capsid. The observations garnered from these ejection experiments reveal (broadly speaking) a picture in which the forces responsible for the ejection process decay as a function of packaged length in the same way as the forces that build up during the packaging process depend on the packaged length, i.e., a reduction in charge increases the speed of ejection. However, the available ejection data only reflect measurements obtained under a few ionic conditions.

It is also possible to measure the force exerted by the DNA inside phage capsids during ejections by inducing phages to eject their DNA into a series of increasingly osmotically resistive solutions (15). By varying the concentration of an osmolyte, such as polyethylene glycol (PEG), one can also vary the resistive pressure. One can therefore measure the amount of DNA inside the phage capsid as a function of external pressure, and hence determine how much force is generated by the DNA inside the capsid as a function of genome length (16–18). It has been proposed that the DNA self-repulsion force can help push the DNA

Submitted March 1, 2010, and accepted for publication June 9, 2010.

△David Wu and David Van Valen contributed equally to this work.

*Correspondence: phillips@pboc.caltech.edu

Editor: Laura Finzi.

0006-3495/10/08/1101/9 $2.00

doi: 10.1016/j.bpj.2010.06.024

into the bacterial cytoplasm (19), but a consensus has yet to be reached. Alternative models propose that highly osmotic environments serve as a condensing agent for DNA exiting phage and actually promote ejection (18,20). Others posit that the osmotic difference (21) between the intra- and extracellular environment is sufficient to flush DNA from the phage into the host (22). However, when certain experimental conditions are met, an increase in the external pressure of the solution can inhibit phage ejections (20). To our knowledge, a systematic study of how different salt conditions influence ejections at different resistive pressures and velocities has yet to be undertaken.

Another way to study ejection and packaging is to look at the structure of the DNA itself inside the capsid. Cryoelectron tomography experiments in which the packaging process of phage $\phi 29$ was paused by freezing have provided information on the structure of viral DNA as a function of length of DNA inside the capsid (23). Other studies have investigated T5 (24,25), λ (26,27), T3 (28), and P22 (29). Recently, the interaxial spacing of condensed DNA was measured as a function of salts to corroborate viral DNA packaging theory (30).

The four experimental techniques described above have shed light on the forces, dynamics, and structure of DNA entering and leaving the viral capsid, and have been complemented by vigorous modeling efforts. These include simple structural models that take into account bending energies and in vitro measurements of electrostatic repulsion (31,33–35), density functional theory with few structural constraints that takes into account electrostatic repulsion/correlations and van der Waals forces (36), and molecular mechanics (23,37,38). This body of work deepens our physical understanding of the packaging and ejection process.

In this work, we focus on the measurement of velocity and force of DNA ejection in bacteriophage λ as a function of charge at fixed ionic strength. In previous experiments (described above), it was shown that ejections occur more slowly in the presence of magnesium as opposed to sodium (13); however, those experiments were not performed at fixed ionic strength, which made it difficult to discern the role of other ion-specific factors, such as charge. Our results demonstrate that the ionic composition controls the observed velocity and force, rather than the ionic strength. We thus propose that the charge of the counterion species is an important control parameter for this system.

We also examined looped ejections, a type of ejection that was not analyzed in previous experiments and was assumed to be an artifact (13). In these ejections, the first portion of the DNA exiting the capsid is stuck at the site of origin, leading to a very bright piece of DNA. This attachment is eventually broken by the flow, fully unfolding the DNA. We demonstrate that looped ejections exhibit the same dynamics as unlooped ejections, and that they are another ejection class rather than an artifact. We confirm this with the use of optical traps. Finally, we provide technical improvements on the single-phage ejection assay, in particular showing that low dye concentrations are necessary to avoid spurious (non-LamB-induced) ejections.

MATERIALS AND METHODS

Phage purification

As a first step, λ phage strain λcI60 was purified according to the method of Sambrook and Russell (39). Briefly, stock phages were amplified by one round of plate lysis and one round of liquid phase lysis, followed by precipitation in PEG. The samples were then purified on a CsCl gradient followed by isopycnic centrifugation. Phages were dialyzed into the appropriate salt condition before use.

LamB purification

The membrane protein LamB was purified using a modified version of a protocol of Keller et al. (40). The *Escherichia coli* strain pop154 was grown overnight in LB + 0.2% maltose at 37°C. The cells were pelleted at 3000 *g* at 4°C for 30 min and resuspended in 50 mM sodium phosphate pH 7.5, 100 mM NaCl, 2 mM EDTA, 5% sucrose. The resuspended cells were subsequently lysed in a French press. The lysate was again centrifuged at 5000 *g* at room temperature for 10 min. The supernatant was collected and the outer membrane fraction was pelleted by ultracentrifugation at 30,000 rpm in a Beckman Ti-60 rotor (Brea, CA) at 18°C for 40 min. The pellet containing the membranes was resuspended in 20 mM sodium phosphate, pH 7.5, and 0.5% octylpolyoxyethylene (oPOE) to extract nonspecific membrane proteins. The solution was incubated in a heat bath at 40°C for 50 min and again pelleted by ultracentrifugation. LamB was extracted by resuspending the pellet in 20 mM sodium phosphate, pH 7.5, and 3% oPOE, incubating at 37°C for 40 min, and pelleting the resulting mixture by ultracentrifugation. The supernatant was dialyzed to 20 mM sodium phosphate, pH 7.5, and 1% oPOE, and then loaded onto a GE MBPTrap column and eluted with 20 mM sodium phosphate, pH 7.5, 1% oPOE, and 20 mM maltose after washing twice with the same solution without maltose. The LamB solution was then dialyzed with 50 mM Tris, pH 7.5, 10 mM $MgSO_4$ (TM), and 1% oPOE. The resulting solution was diluted to 2 mg/mL. The concentration was assayed by measuring the absorbance at 280 nm, and the purity was verified by sodium dodecyl sulfate polyacrylamide gel electrophoresis.

Single phage ejection assay

For the single phage ejection assay, we followed a protocol developed by Mangenot et al. (12) and Grayson et al. (13) (Fig. 1 *A*). Microscope coverslips were cleaned by sonication in 1M KOH for 10 min, followed by sonication in water for 10 min, and dried on a hot plate. Glass slides were drilled using a diamond-covered drill bit, and 5 inches of tubing was attached to the glass slide with epoxy. The flow chamber was assembled using laser-cut, double-sided adhesive tape (41). A solution of 10^8–10^{11} pfu/mL λ phage and 20 nm fluorescent polystyrene beads (focusing aids) was incubated in the assembled flow chambers for 10 min. Once focused, the chamber was washed with 200 μL of buffer + 1% oPOE. The buffers had the following ionic compositions: 0, 2.5, 5, 7.5, or 10 mM NaCl and 2.5, 1.875, 1.25, 0.625, or 0 mM MgSO4, respectively, in addition to 10 mM Tris, pH 7.5. The solution to induce ejection consisted of buffer, 1% oPOE, 1% glucose oxidase/catalase, 10^6 diluted SYBR gold, and 1% LamB. Occasionally, 20 μg/mL acetylated bovine serum albumin, 3 mg/mL casein, and 80 μg/mL heparin were added to the buffer to block the glass surface and determine whether looping ejections disappeared. Calibration of lengths was performed as described previously (13).

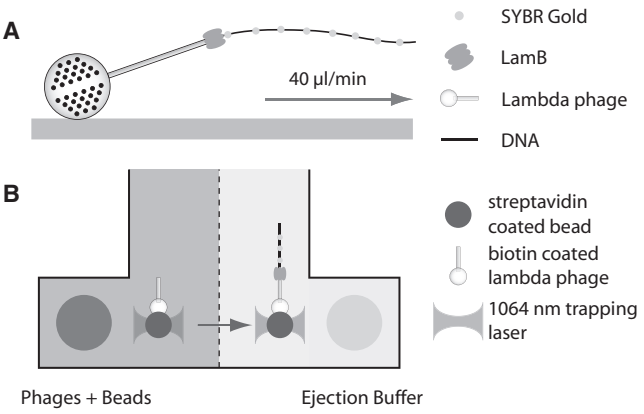

FIGURE 1 Schematics for observing DNA ejection by single phage λ virions in vitro. DNA was visualized using fluorescence microscopy. (*A*) Ejection at a surface. A flow chamber was incubated with λ phage and the viruses were allowed to nonspecifically settle onto the surface. DNA ejection was triggered by flowing in LamB, and the ejected DNA was visualized using SYBR gold. The flow field extends the ejected DNA, allowing quantification of the amount of DNA ejected by either measuring the length in pixels or measuring the total intensity. (*B*) Ejection on a bead. A parallel ejection assay using an optical trap was developed. Biotinylated phages were bound to streptavidin-coated polystyrene beads. A dual-input flow chamber was used. Beads coated with λ phage entered the chamber through one input and an ejection buffer consisting of LamB and SYBR gold entered through the other. In the presence of flow, the two fluids are well separated. An optical trap was used to move a phage-coated bead into the ejection buffer to initiate DNA ejection.

Microscopy

Samples were imaged at 60X and 100X using a Nikon perfect focus system (Nikon, Melville, NY) and either a SYBR gold or FITC filter set. Images were acquired with a Photometrics CoolSnap ES2 camera (Tucson, AZ), with an exposure time of 75 ms and frame rate of ~4 fps.

Image analysis

A custom segmentation algorithm was developed with the use of MATLAB (The MathWorks, Natick, MA). Ejection events were identified in each movie by local adaptive thresholding on the fluorescence intensity. DNA was identified in each ejection by using background subtraction, median and Wiener filters for denoising, and a custom Canny filter for edge-finding. The long-axis length, total intensity, and background (the mean intensity of non-DNA-related pixels) were extracted for each ejection. Trajectories were subjected to a three-bin median filter for denoising.

Force dependence assay

For the force dependence assay, we followed a protocol adapted from Evilevitch et al. (15). Phages were quickly swirled in a solution of 1% oPOE, 1% LamB, 1% DNase, and appropriate buffer containing PEG at 37°C and incubated for 1 h at 37°C (17). The solution was then incubated in a 65°C water bath for 50 min to break open capsids and inactivate DNase. DNA in capsids was then extracted by a 1:1 phenol/chloroform extraction followed by chloroform extraction and finally ethanol precipitation. DNA lengths were assayed using field inversion agarose gel electrophoresis (100 V forward 0.8 s, 60 volts backward 0.8 s, for 7–10 h). After staining with ethidum bromide, migration distance was quantified using MATLAB.

Optical trapping

Phages were biotinylated after a standard plate lysis by incubation with 10 μM of sulfo-LC-biotin, after they were first dialyzed for 48 h with 100 mM sodium bicarbonate, pH 8.2 (see Fig. 1 *B*). The phages were then purified on a CsCl gradient. The biotinylated phages were incubated with 2 μm streptavidin-coated polystyrene spheres for a few hours at room temperature on a rotating rack. The streptavidin spheres were washed by resuspension in TM three times and diluted 10-fold into TM during use. The phage ejection solution (see "Single phage ejection assay" above) was injected into one port, and the phages conjugated to streptavidin spheres were injected into the other port at 10 μL/min. A 1064 nm laser at 100 mW was used to trap phage-bound spheres, which were moved across the boundary layer of the two solutions. The microscope was built in-house around a 60X IR-corrected water immersion objective adapted with a 200 mm focal length tube lens, and imaged with an Andor Ixon EMCCD camera (Andor, South Windsor, CT). The schematic of the chamber shown in Fig. 1 *B* was adapted from Brewer and Bianco (41).

RESULTS AND DISCUSSION

Our first set of experiments focused on optimizing the single phage ejection assay with regard to SYBR gold concentration, since we noticed that phages spontaneously eject their DNA in high concentrations of SYBR gold. SYBR gold is thought to affect the mechanical properties of DNA, since other DNA stains have been shown to affect DNA's persistence length (42). To investigate the origin of these ejections and to test the hypothesis that they are triggered by SYBR gold, we incubated phages in different salts and different amounts of SYBR gold, and subsequently measured the number of active phages by titering. The results are given in Table 1; errors in the titer values follow $\sqrt{N}$ (counting) statistics. For high amounts of SYBR gold (1:10,000), we see a steep drop in the number of active phages, between 2- and 10-fold for the buffers containing magnesium. The drop is particularly drastic in pure sodium (1000-fold), a condition that is believed to increase the DNA pressure inside the capsid. One possible explanation for this is that sodium in concert with SYBR gold increases the DNA pressure enough to destabilize the phage. Alternatively, magnesium and SYBR gold could compete with each other for binding sites on the DNA, providing a protective effect. Another possibility is that SYBR gold acts by a mechanism similar to that of LamB (see the Supporting Material for more details). Regardless, the drop in titer is consistent with the hypothesis that SYBR gold induces ejections. When the SYBR gold concentration was reduced (1:1,000,000), we recovered almost the entirety of the original titer value. We concluded that it was preferable to perform the experiment at this lower concentration to minimize the effect of SYBR gold. The concomitant reduction in signal did not affect our DNA segmentation algorithms.

When performing the single phage ejection assay (Fig. 1 *A*), we always noticed two types of ejections: ejections that looked similar to those previously reported, and ejections that revealed a different type of dynamics, with the appearance of a partial ejection, and were previously

TABLE 1 Phage survival in SYBR gold

Ionic composition	Titer ($\times 10^{11}$)	Titer in high SYBR ($\times 10^{11}$)	Titer in low SYBR ($\times 10^{11}$)	% looped in low SYBR with LamB	% looped in low SYBR with no LamB
50 mM Tris 10 mM Mg 0 mM Na	1	0.41	0.55	88	35
10 mM Tris 2.5 mM Mg 0 mM Na	0.76	0.07	0.59	58.8	13.2
10 mM Tris 1.875 mM Mg 2.5 mM Na	0.90	0.10	0.86	57.6	25
10 mM Tris 1.25 mM Mg 5 mM Na	0.79	0.03	0.97	50	48
10 mM Tris 0.625 mM Mg 7.5 mM Na	0.93	0.08	1.10	44.9	20
10 mM Tris 0 mM Mg 10 mM Na	0.69	0.001	0.55	55.3	6.9

SYBR gold triggers DNA ejection independent of LamB; the presence of LamB influences the character of ejection. Columns 1–3: Titers of phage λ solutions as a function of buffer composition and SYBR gold concentration. CsCl purified λ phage were dialyzed in the appropriate buffer by washing and spin filtering. SYBR gold was added to bring the solution to the right concentration (none, high (1:10,000), and low (1:1,000,000)). The number of viable phage remaining was measured by titering. High concentrations of SYBR gold reduce the titer by more than an order of magnitude, especially in the absence of magnesium, because SYBR gold induces the bacteriophage to eject their DNA. Lowering the concentration of dye recovers the original titer levels. Columns 4 and 5: Character of ejection in the presence and absence of LamB. A single phage ejection assay was run for each condition with and without LamB. The number of ejections, both continuous and looped, was counted manually and is reported above. The fraction of ejections that are looped is higher in the presence of LamB.

viewed as artifactual (13) (see Fig. 3 *A*). Furthermore, we always saw spurious ejections of both types, as indicated in Table 1 (last column). In our investigations into the origins of the spurious ejections, we found that under certain salt conditions (Table 1), we saw more "artifactual" ejections after addition of LamB (up to a threefold increase) in the single phage ejection assay. This led us to question their designation as artifacts.

However, it is well known that DNA will stick to glass beads (43), and the previous experiment does not rule out the possibility that DNA was sticking to the microscope coverslip. However, this seems unlikely, since the addition of LamB (in excess) would tend to block sites on the glass for the ejecting DNA to bind to. We confirmed the stickiness of the glass by incubating λ phage DNA on freshly cleaned coverslips; upon observation, the glass was covered in DNA (data not shown). As another test, therefore, we performed the ejection assay in the presence of the surface blocking agents BSA, casein, and heparin. These blocking agents significantly reduced DNA's affinity to the surface (44). When bare λ DNA was again incubated in a flow chamber with these blocking agents, only a single strand was found after extensive searching efforts (data not shown). However, even with these blocking agents, the so-called artifactual ejections were seen in the phage ejection assay. Fortunately, the content of the artifactual ejections could be deduced from serendipitous ejections: occasionally, it could be seen that the DNA was in fact in a looped state. This was quantified by an intensity histogram and is shown in Fig. 2 *A*. We therefore term this class "looped ejections," in contrast to the ejections previously characterized, which we call continuous ejections. The addition of LamB tends to increase the amount of looped ejections (Table 1), which suggests that looped ejections are physiological.

We attempted to further mitigate surface effects by ejecting biotinylated phages off of optically trapped 2 μm (Movie S1) and 500 nm (data not shown) streptavidin-coated polystyrene spheres in the presence of surface blocking agents. A dual-syringe pump was used to push fluid into the chamber (Fig. 1 *B*). Using an optical trap, we grabbed hold of a microsphere and moved it across the laminar flow boundary layer into the ejection buffer. The continuous flow system limits diffusive mixing at the meeting juncture. After a LamB trimer finds its target, a phage ejects and we can monitor the ejection (Fig. 2 *B*). We found that the looped ejections were as common as continuous ejections. These experiments support the hypothesis that loops occur when the exiting DNA sticks to the LamB or the phage capsid, as may be the case in phage T5 (14).

We next characterized the dynamics of both the looped and continuous ejections under different ionic compositions, again using low concentrations of SYBR gold as described above (Fig. 1 *A*). We first flowed in the dye front to visualize any spontaneous or SYBR gold-induced ejections. Even at a 10-fold lower concentration of SYBR than previously reported (13), there were still some spurious ejections, albeit much less than would occur with the SYBR gold concentrations used previously (13). Any lower concentration of dye would have precluded accurate segmentation of the ejecting DNA. After a period of time during which the rate of spurious ejections was observed to be steady, we added LamB to the solution. A sudden large increase in the rate of visualized ejections indicated that LamB was inducing a large fraction of subsequent ejections. However, it should be noted that the dynamics of ejections induced by SYBR gold and those induced by LamB are indistinguishable. The experiment was repeated for five different salt conditions in which we systematically varied the amount of sodium and magnesium ions while keeping the ionic strength constant.

We analyzed as many ejections within a field of view as possible. Reasons for excluding an ejection from analysis included overlapping with another ejecting phage, photodamage during an ejection, or a looped ejection that did

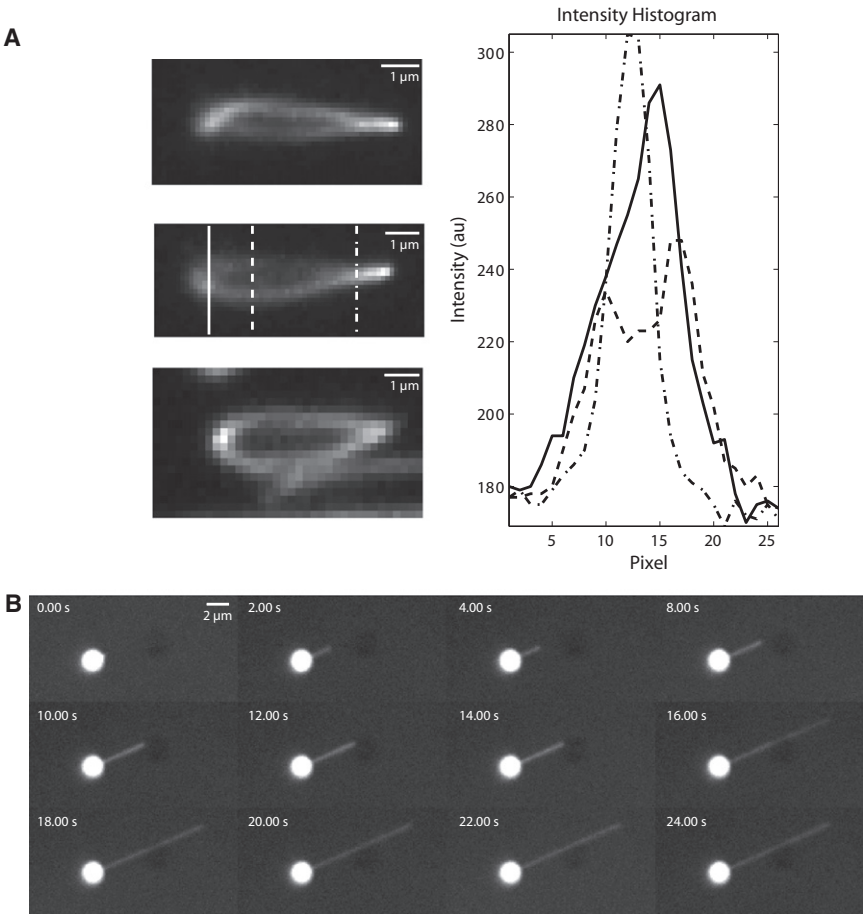

FIGURE 2 Looping during DNA ejection. (*A*) A montage of loops observed during the single phage ejection assay. An intensity histogram constructed from one of the examples demonstrates the presence of loops during in vitro ejections. (*B*) Montage observation of a looped ejection during an optical trapping experiment. Phages were ejected off of optically trapped beads to suppress effects caused by the surface. Looped ejections are still observed, suggesting that they are not the byproduct of surface effects. The bead is 2 μm in diameter.

not completely unfold. Ejections extracted from the field of view were partitioned into two categories: continuous and looped. These are highlighted in Fig. 3, *A* and *B*, respectively. To quantify the dynamics, we designed a custom segmentation algorithm for the DNA strands. We determined the relation between the length of DNA in base-pairs and in pixels by measuring, under flow, different known lengths of λ DNA cut with restriction enzymes, and fitting the result to a quadratic function (see Fig. S1). This calibration deconvolutes polymer stretch and shear flow from the actual DNA length (46). The DNA's long-axis length for each time point in a trajectory was then interpolated according to a quadratic function and normalized by 48.5 kbp, the full length of λ phage DNA. This calibration is only accurate for continuous ejections; for looped ejections, it is necessary to use intensity to discern the amount of DNA ejected. To do so, we take the total intensity of the DNA above background and normalize by the maximum intensity observed in a trajectory. This was done for both continuous and looped ejections (Fig. 3, *C* and *D*; Fig. S2, *A–E*).

A representative example of the trajectories is shown in Fig. 3, *C* and *D*, and trajectories for each ionic condition are shown in Fig. S2, *A–E*. The fraction of DNA ejected is plotted versus time. The green curve uses fluorescence intensity to quantify total DNA ejected, whereas the blue curve uses the calibrated length. It is clear in the looped trajectories that the DNA is in fact pinned at one end, as the trajectories exhibit a discontinuity in length at half-maximal ejection. A comparison of results obtained using calibrated DNA lengths or intensity as a measure of total ejected DNA is shown in Fig. S3, *A–E*. Intensity measures give a larger estimate for the velocity of DNA ejected at early times because our segmentation algorithm misses the first bits of DNA ejection. Thus, changes in DNA length appear relatively large at small lengths, whereas at late stages in the ejection, length and intensity measures are equivalent metrics for the amount of DNA ejected.

For each condition, we binned the trajectories to compute the average velocity as a function of DNA remaining in the capsid. This is plotted in Fig. 3, *E* and *F*. Fig. 3 *E* was computed using calibrated length, and Fig. 3 *F* was computed using intensities. Velocity plots for individual salt conditions are shown in Fig. S4, *A–E*. From our analysis of the dynamics, we observed that individual trajectories were very similar to each other. In agreement with previous work (13), this leads us to conclude that we are observing the same intrinsic dynamical process and that differences between trajectories are likely the result of measurement error. In addition, our systematic perturbation of the sodium

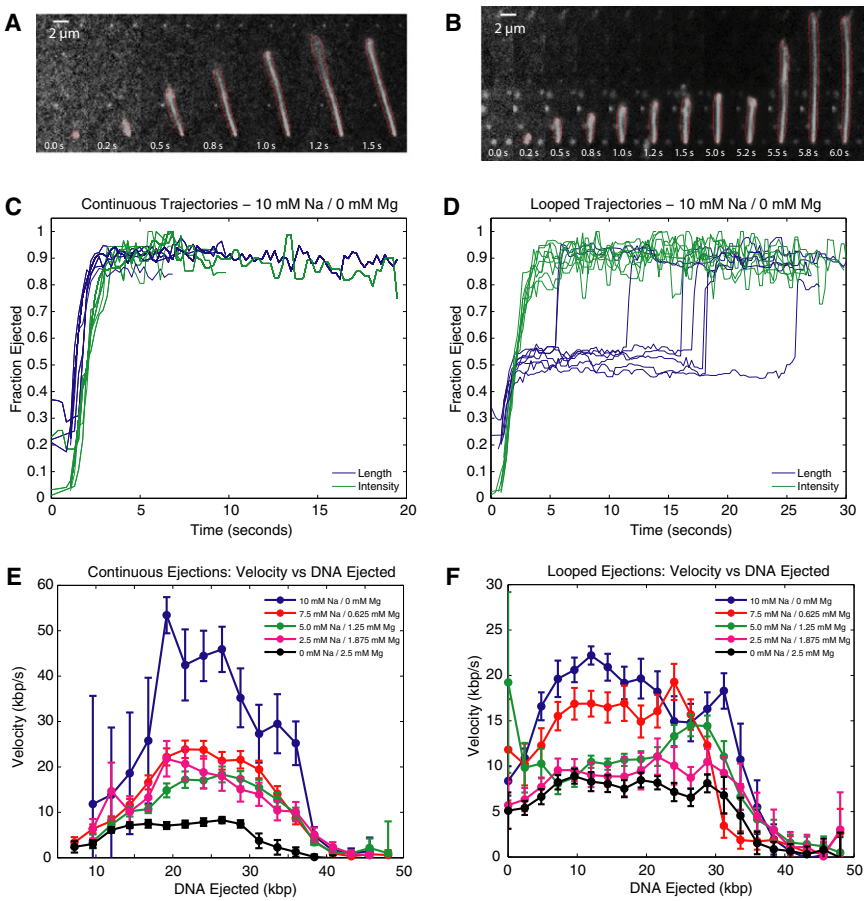

FIGURE 3 Trajectories of single phage ejections and the ion-concentration dependence of the ejection dynamics. (*A* and *B*) Montage of (*A*) continuous and (*B*) looped ejections in movies of individual phages ejecting their DNA. The identified pieces of DNA are outlined. (*C* and *D*) Sample trajectories for (*C*) continuous and (*D*) looped ejections. The amount of DNA ejected was quantified by measuring either the calibrated long-axis length or the total intensity above background of the segmented region. Lengths were determined by calibrating against restriction enzyme digested λ DNA at known lengths, as described in the text. Individual trajectories are normalized by 48.5 kbp, the maximum genome length, or the maximum intensity observed during an individual trajectory to obtain the fraction ejected. Two qualitatively different ejections—continuous and looped—are observed. The looped ejections reach half-maximal length before unfolding. The total intensity provides a way to quantify the total amount of DNA outside the capsid. (*E* and *F*) The velocity of ejection is shown as a function of buffer composition for (*E*) continuous and (*F*) looped trajectories. For each trajectory, the velocity of the DNA (measured using total intensity) at different landmark lengths was recorded. The mean velocity and the standard error of the DNA at each landmark length are plotted for each buffer condition. There is a clear trend in the data: buffers with more magnesium ions have a longer timescale for DNA ejection. Continuous and looped ejections have similar ejection dynamics in all buffer conditions. See online version for color.

and magnesium concentrations (at fixed ionic strength) showed a consistent trend. As the amount of magnesium was lowered and the amount of sodium was increased, the speed of the ejections increased (Fig. 3, *E* and *F*). From this, we conclude that it is the type, rather than the amount, of ion present that is an important control parameter in governing DNA ejection dynamics. We posit that the role of the positive ions is to screen the negative charge of the DNA backbone, which suggests that the charge of the counterions is the property of interest.

Additionally, we observe that the continuous and looped ejections have velocity curves that are within error of each other (Fig. 3, *E* and *F*). This suggests that the ejection mechanisms for these two classes of ejections are very similar, if not identical, and that what happens to the first segment of DNA that exits the capsid determines whether an ejection will be continuous or looped.

To continue the physical characterization of the ejection process, we performed osmotic suppression experiments to determine the forces that drive ejection in each of the different salt conditions. It has been reported that osmotic pressure varies with PEG 8000 concentration (47). Previous experiments have measured the amount of DNA ejected by pelleting phage capsids and measuring the absorbance at 260 nm. This measures the amount of DNA that has been consumed by the DNase. The mass of ejected DNA is thus accurately measured; however, the relation between the mass of ejected DNA and the length of DNA remaining in the capsid is not straightforward, as the fraction of phages that eject may vary for each PEG concentration. Previous experiments suggest that the fraction of phages that eject is constant for phage λ (16); however, it has been demonstrated that this is not true for SPP1 and may not be true for other phage species (see Supporting Material) (48). To circumvent this issue, we purified the DNA inside the capsids by standard extraction techniques and measured its length directly by using field inversion gel electrophoresis (Fig. S5) (15). Care was taken to avoid centrifugation, as it tends to fragment DNA (data not shown). The pressure driving ejection is shown in Fig. 4 *A*. The general trend is that decreasing magnesium and increasing sodium increases the driving force, although the 5, 7.5, and 10 mM Na samples appear to be within error of each other. We observed that up to 65 atmospheres (~30 pN) of pressure was not enough to stall ejections in some salt conditions, which is consistent with theoretical expectations (13) and previous experimental observations (49). Atmospheres can be converted to force

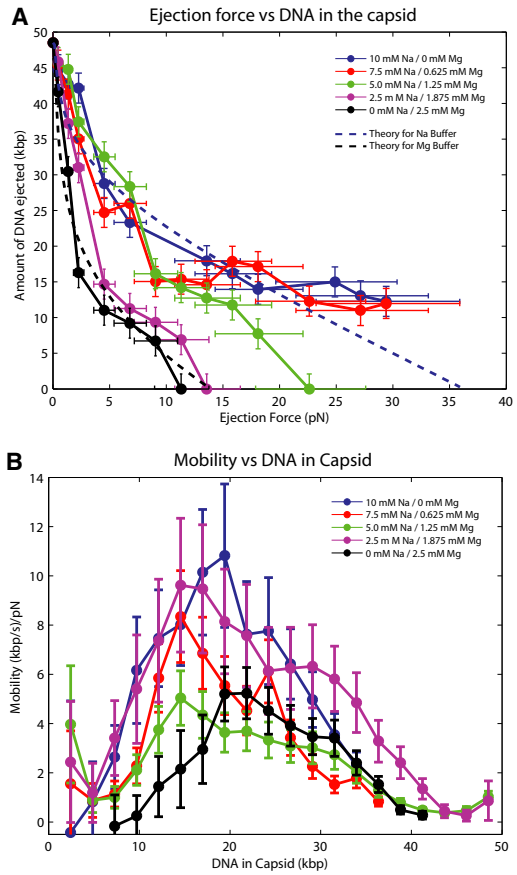

FIGURE 4 The force that drives DNA ejection. Osmotic suppression experiments were performed in different buffer conditions to measure the force that drives ejection. The fraction of DNA ejected was determined by measuring the amount of capsid DNA remaining using field inversion gel electrophoresis. (*A*) Increasing monovalent ion concentration raises the stall force of ejection at each length of DNA. Dotted lines are theoretical predictions according to Grayson et al. (13). (*B*) The mobility is measured as $v(l)/F(l)$. The trend is less clear regarding mobility and ion composition, although it appears that mobility is independent of ion composition for constant ionic strength. Vertical error bars were determined by the electrophoresis resolution, which was ± 2.1 kbp; horizontal error bars were determined by the pipetting accuracy of the PEG solutions, which had up to 5% variability. See online version for color.

by multiplying the pressure by the end-on area of DNA, assuming a radius of 1.2 nm (17). On top of the data are plotted theoretical predictions of the fraction ejected (13) as a function of pressure for 10 mM Na, 0 mM Mg, and 0 mM Na, 2.5 mM Mg, given the parameters determined by Rau et al. (50). The theory, which assumes crystalline packing of DNA inside the capsid with intrastrand repulsive forces determined by the character of the couterions, fits the data quite well.

A simple model posits a linear relation between net forces and velocity, captured by the friction coefficient or its inverse, mobility. We can determine how the mobility, denoted by $\sigma(l)$, of DNA inside the capsid depends on the salts (Fig. 4 *B*), such that $F(l) = v(l)/\sigma(l)$, where l is the DNA length in the capsid, F is the force as measured in Fig. 4 *A* (multiplied by the area of end-on DNA), and v is the velocity as measured in Fig. 3, *E* and *F*. This calculation assumes that the ejection is quasistatic; we assume that the DNA inside the capsid during the single-phage ejection experiments has relaxed to the equilibrium configuration in the osmotic suppression experiments. As previously observed (13), the mobility depends strongly on the amount of DNA remaining in the capsid. As the two extreme salt conditions overlap in Fig. 4 *B* at increased DNA inside the capsid, we are unable to conclude that mobility is dependent on ion character at constant ionic strength.

CONCLUSIONS

We investigated the dynamics of DNA ejection in a variety of different salts, and also performed measurements on the self-repulsive force driving this process. We demonstrated that the counterion charge is an important control parameter for this class of experiments. These measurements should be of use to theorists working in the field of physical virology. Of particular interest would be the development of models that can predict the force that will drive ejection in different salts, as well as a better understanding of the timescale of the ejection process. We also investigated the origin of looped ejections. On the basis of our data, we can propose several possible models for these processes. It is possible that the end of the DNA gets stuck on the tail of the phage or LamB as it comes out, and that the rest of the genome subsequently comes out of the tail, accounting for the DNA loops occasionally seen (Fig. 2 *A*). This may make it possible for phage to circularize even faster as the genome rushes to get inside its host, *E. coli*, as it is theorized that λ delivers its genome directly into the cytoplasm without going through the periplasmic space (51). Although looped ejections were first observed in 2007 (13), this is the first attempt (to our knowledge) to explain this phenomenon.

Of particular note is the relation of our work to that of Fuller et al. (10). In their investigation of the packaging process as a function of salts, they noted that when the amount of multivalent cations in the packaging assay was increased, the virus packaged faster and required less force at an equivalent fraction of DNA packaged. This suggests that increasing magnesium reduces the amount of intrastrand DNA repulsion. We see a similar effect in our study; i.e., an increased force is required to stall ejecting DNA at the same length, with increased monovalency. However, the mobility during DNA ejection appears to be independent of salt composition at our detection resolution. Notably, the speed of ejection is faster during ejection in the presence of larger fractions of monovalent cations, which is consistent with the packaging data. Altogether, the results presented here represent a step forward in understanding the forces at play when bacteriophage λ infects bacteria.

SUPPORTING MATERIAL

Five figures, one movie, and additional references are available at http://www.biophysj.org/biophysj/supplemental/S0006-3495(10)00736-8.

The authors thank the members of the physiology course at the Marine Biology Laboratory in Woods Hole, MA (Nicolas Chiaruttini, Paul Grayson, Zenan Chang, Alexander Grosberg, Ian Molineux, Michael Rubinstein, Virgile Viasnoff, William Gelbart, and Charles Knobler), and members of the Phillips laboratory.

D.W. and D.V.V. were supported by a National Institutes of Health (NIH) Medical Scientist Training Program Fellowship. D.V.V. was supported by a Yaser Abu-Mostafa Hertz Fellowship and an NIH Director's Pioneer Award. R.P., D.W., and D.V.V. were supported by National Science Foundation grant No. 0758343 and an NIH Pioneer Award. Q.H. was supported by a predoctoral fellowship (BC083077) from the Department of Defense Breast Cancer Research Program.

REFERENCES

1. Hershey, A. D., and M. M. Chase. 1952. Independent functions of viral protein and nucleic acid in growth of bacteriophage. *J. Gen. Physiol.* 36:39–56.
2. Smith, G. P. 1991. Surface presentation of protein epitopes using bacteriophage expression systems. *Curr. Opin. Biotechnol.* 2:668–673.
3. Catalano, C. E., D. Cue, and M. Feiss. 1995. Virus DNA packaging: the strategy used by phage λ. *Mol. Microbiol.* 16:1075–1086.
4. Smith, D. E., S. J. Tans, …, C. Bustamante. 2001. The bacteriophage straight ϕ29 portal motor can package DNA against a large internal force. *Nature.* 413:748–752.
5. Oppenheim, A. B., O. Kobiler, …, S. Adhya. 2005. Switches in bacteriophage λ development. *Annu. Rev. Genet.* 39:409–429.
6. Arkin, A., J. Ross, and H. H. McAdams. 1998. Stochastic kinetic analysis of developmental pathway bifurcation in phage λ-infected *Escherichia coli* cells. *Genetics.* 149:1633–1648.
7. St-Pierre, F., and D. Endy. 2008. Determination of cell fate selection during phage λ infection. *Proc. Natl. Acad. Sci. USA.* 105: 20705–20710.
8. Zeng, L., S. O. Skinner, …, I. Golding. 2010. Decision making at a subcellular level determines the outcome of bacteriophage infection. *Cell.* 141:682–691.
9. Dodd, I. B., K. E. Shearwin, and J. B. Egan. 2005. Revisited gene regulation in bacteriophage λ. *Curr. Opin. Genet. Dev.* 15:145–152.
10. Fuller, D. N., J. P. Rickgauer, …, D. E. Smith. 2007. Ionic effects on viral DNA packaging and portal motor function in bacteriophage ϕ29. *Proc. Natl. Acad. Sci. USA.* 104:11245–11250.
11. Novick, S. L., and J. D. Baldeschwieler. 1988. Fluorescence measurement of the kinetics of DNA injection by bacteriophage λ into liposomes. *Biochemistry.* 27:7919–7924.
12. Mangenot, S., M. Hochrein, …, L. Letellier. 2005. Real-time imaging of DNA ejection from single phage particles. *Curr. Biol.* 15:430–435.
13. Grayson, P., L. Han, T. Winther, and R. Phillips. 2007. Real-time observations of single bacteriophage λ DNA ejections in vitro. *Proc. Natl. Acad. Sci. USA.* 104:13652–14657.
14. Chiaruttini, N., M. de Frutos, …, V. Viasnoff. 2010. Is the in vitro ejection of bacteriophage DNA quasi-static? A bulk to single virus study. *Biophys. J.* 99:447–455.
15. Evilevitch, A., L. Lavelle, …, W. M. Gelbart. 2003. Osmotic pressure inhibition of DNA ejection from phage. *Proc. Natl. Acad. Sci. USA.* 100:9292–9295.
16. Evilevitch, A., J. W. Gober, …, W. M. Gelbart. 2005. Measurements of DNA lengths remaining in a viral capsid after osmotically suppressed partial ejection. *Biophys. J.* 88:751–756.
17. Grayson, P., A. Evilevitch, …, R. Phillips. 2006. The effect of genome length on ejection forces in bacteriophage λ. *Virology.* 348:430–436.
18. Leforestier, A., S. Brasilès, …, F. Livolant. 2008. Bacteriophage T5 DNA ejection under pressure. *J. Mol. Biol.* 384:730–739.
19. Kindt, J., S. Tzlil, …, W. M. Gelbart. 2001. DNA packaging and ejection forces in bacteriophage. *Proc. Natl. Acad. Sci. USA.* 98: 13671–13674.
20. Jeembaeva, M., M. Castelnovo, …, A. Evilevitch. 2008. Osmotic pressure: resisting or promoting DNA ejection from phage? *J. Mol. Biol.* 381:310–323.
21. Stock, J. B., B. Rauch, and S. Roseman. 1977. Periplasmic space in *Salmonella typhimurium* and *Escherichia coli*. *J. Biol. Chem.* 252:7850–7861.
22. Molineux, I. J. 2006. Fifty-three years since Hershey and Chase; much ado about pressure but which pressure is it? *Virology.* 344:221–229.
23. Comolli, L. R., A. J. Spakowitz, …, K. H. Downing. 2008. Three-dimensional architecture of the bacteriophage ϕ29 packaged genome and elucidation of its packaging process. *Virology.* 371:267–277.
24. Leforestier, A., and F. Livolant. 2009. Structure of toroidal DNA collapsed inside the phage capsid. *Proc. Natl. Acad. Sci. USA.* 106:9157–9162.
25. Leforestier, A., and F. Livolant. 2010. The bacteriophage genome undergoes a succession of intracapsid phase transitions upon DNA ejection. *J. Mol. Biol.* 396:384–395.
26. Evilevitch, A. 2006. Effects of condensing agent and nuclease on the extent of ejection from phage λ. *J. Phys. Chem. B.* 110:22261–22265.
27. Hud, N. V., and K. H. Downing. 2001. Cryoelectron microscopy of λ phage DNA condensates in vitreous ice: the fine structure of DNA toroids. *Proc. Natl. Acad. Sci. USA.* 98:14925–14930.
28. Fang, P. A., E. T. Wright, …, W. Jiang. 2008. Visualization of bacteriophage T3 capsids with DNA incompletely packaged in vivo. *J. Mol. Biol.* 384:1384–1399.
29. Johnson, J. E., and W. Chiu. 2007. DNA packaging and delivery machines in tailed bacteriophages. *Curr. Opin. Struct. Biol.* 17: 237–243.
30. Evilevitch, A., L. T. Fang, …, C. M. Knobler. 2008. Effects of salt concentrations and bending energy on the extent of ejection of phage genomes. *Biophys. J.* 94:1110–1120.
31. Odijk, T. 1998. Hexagonally packed DNA within bacteriophage T7 stabilized by curvature stress. *Biophys. J.* 75:1223–1227.
32. Reference deleted in proof.
33. Purohit, P. K., J. Kondev, and R. Phillips. 2003. Mechanics of DNA packaging in viruses. *Proc. Natl. Acad. Sci. USA.* 100:3173–3178.
34. Tzlil, S., J. T. Kindt, …, A. Ben-Shaul. 2003. Forces and pressures in DNA packaging and release from viral capsids. *Biophys. J.* 84: 1616–1627.
35. Purohit, P. K., M. M. Inamdar, …, R. Phillips. 2005. Forces during bacteriophage DNA packaging and ejection. *Biophys. J.* 88:851–866.
36. Li, Z., J. Wu, and Z. G. Wang. 2008. Osmotic pressure and packaging structure of caged DNA. *Biophys. J.* 94:737–746.
37. Petrov, A. S., and S. C. Harvey. 2007. Structural and thermodynamic principles of viral packaging. *Structure.* 15:21–27.
38. Petrov, A. S., and S. C. Harvey. 2008. Packaging double-helical DNA into viral capsids: structures, forces, and energetics. *Biophys. J.* 95:497–502.
39. Sambrook, J., and D. W. Russell. 2001. Molecular Cloning: A Laboratory Manual. Cold Spring Harbor Laboratory Press, Cold Spring Harbor, New York.
40. Keller, T. A., T. Ferenci, …, J. P. Rosenbusch. 1994. Crystallization of monodisperse maltoporin from wild-type and mutant strains of various Enterobacteriaceae. *Biochem. Biophys. Res. Commun.* 199:767–771.
41. Brewer, L. R., and P. R. Bianco. 2008. Laminar flow cells for single-molecule studies of DNA-protein interactions. *Nat. Methods.* 5: 517–525.

42. Smith, D. E., T. Perkins, and S. Chu. 1996. Dynamical scaling of DNA diffusion coefficients. *Macromolecules.* 29:1372–1373.

43. Joly, E. 1996. Purification of DNA fragments from agarose gels using glass beads. *In* Methods in Molecular Biology: Basic DNA and RNA protocols. A. J. Harwood, editor. Humana Press, Totowa, NJ.

44. Han, L., H. G. Garcia, …, R. Phillips. 2009. Concentration and length dependence of DNA looping in transcriptional regulation. *PLoS ONE.* 4:e5621.

45. Reference deleted in proof.

46. Marko, J. F., and E. D. Siggia. 1995. Stretching DNA. *Macromolecules.* 28:8759–8770.

47. Michel, B. E. 1983. Evaluation of the water potentials of solutions of polyethylene glycol 8000 both in the absence and presence of other solutes. *Plant Physiol.* 72:66–70.

48. São-José, C., M. de Frutos, …, P. Tavares. 2007. Pressure built by DNA packing inside virions: enough to drive DNA ejection in vitro, largely insufficient for delivery into the bacterial cytoplasm. *J. Mol. Biol.* 374:346–355.

49. Fuller, D. N., D. M. Raymer, …, D. E. Smith. 2007. Measurements of single DNA molecule packaging dynamics in bacteriophage λ reveal high forces, high motor processivity, and capsid transformations. *J. Mol. Biol.* 373:1113–1122.

50. Rau, D. C., B. Lee, and V. A. Parsegian. 1984. Measurement of the repulsive force between polyelectrolyte molecules in ionic solution: hydration forces between parallel DNA double helices. *Proc. Natl. Acad. Sci. USA.* 81:2621–2625.

51. Esquinas-Rychen, M., and B. Erni. 2001. Facilitation of bacteriophage λ DNA injection by inner membrane proteins of the bacterial phosphoenol-pyruvate: carbohydrate phosphotransferase system (PTS). *J. Mol. Microbiol. Biotechnol.* 3:361–370.